POLSKA AKADEMIA NAUK

INSTYTUT MASZYN PRZEPŁYWOWYCH

TRANSACTIONS OF THE INSTITUTE OF FLUID-FLOW MACHINERY

PRACE INSTYTUTU MASZYN PRZEPŁYWOWYCH

104

WYDAWNICTWO IMP PAN

GDAŃSK 1998

THE TRANSACTIONS OF THE INSTITUTE OF FLUID-FLOW MACHINERY

exist for the publication of theoretical and experimental investigations of all aspects of the mechanics and thermodynamics of fluid-flow with special reference to fluid-flow machines

*

PRACE INSTYTUTU MASZYN PRZEPŁYWOWYCH

poświęcone są publikacjom naukowym z zakresu teorii i badań doświadczalnych w dziedzinie mechaniki i termodynamiki przepływów, ze szczególnym uwzględnieniem problematyki maszyn przepływowych

Wydanie publikacji zostało dofinansowane przez PAN ze środków DOT uzyskanych z Komitetu Badań Naukowych

EDITORIAL OFFICE – REDAKCJA

Wydawnictwo Instytutu Maszyn Przepływowych
Polskiej Akademii Nauk
ul. Gen. Józefa Fiszera 14, 80-952 Gdańsk, skr. poczt. 621,
☎ (0-58) 341-12-71 wew. 141, fax: (0-58) 341-61-44,
e-mail: esli@imppan.imp.pg.gda.pl

ISSN 0079-3205

TRANSACTIONS OF THE INSTITUTE OF FLUID-FLOW MACHINERY

No. 104, 1998, 3-18

MAIK TIEDEMANN[1]

Stator wake effects on the total pressure distribution downstream of a transonic turbine rotor

Within a European project which aimed at the investigation of stator wake – rotor blade interactions, measurements were carried out to determine the unsteady pressure distribution downstream of a transonic high pressure turbine stage.

The experiments were conducted in the wind-tunnel for rotating cascades at the DLR Göttingen (RGG). The RGG is a closed loop facility, that enabled real engine Mach and Reynolds numbers in the turbine stage. The stator vanes had coolant ejection slots close to the trailing edge at the pressure side.

A Pitot probe, equipped with a fast response pressure transducer and a common pneumatic pressure tube was installed downstream of the rotor. The measurement position was 0.5 axial rotor chords downstream of the rotor trailing edge at midspan. The stator vane passing frequency as seen by the rotor was 5.6 kHz and the rotor blade passing frequency as seen by the probe was 8.4 kHz. The pneumatic pressure was used as a reference for the rather inaccurate dc-readings of the fast response transducer.

Measurements were carried out for two different coolant ejection rates. Firstly with no coolant ejected and secondly with 3% of the main mass flow ejected.

In the mean values of the total pressure downstream of the stage, the stator wake is clearly visible. The periodic fluctuations of the total pressure downstream of the rotor are about 50% smaller in the region of the stator wake than in the region of undisturbed inlet flow. Thus, the stator wake damps the total pressure fluctuations generated by the rotor.

Nomenclature

a	–	speed of sound,	Re	–	Reynolds number,
c	–	chord, absolute velocity,	srp	–	Stator-Rotor-Probe relative position,
c_m	–	coolant ejection rate,	t	–	time,
M	–	Mach number,	T	–	temperature, period,
N	–	number of revolutions,	w	–	relative velocity,
		rotational speed,	α	–	absolute flow angle,
p	–	pressure,	β	–	relative flow angle,
R	–	gas constant (287 $\frac{\mathrm{J}}{\mathrm{kgK}}$),	η	–	dynamic viscosity,
			κ	–	specific heat ratio (1.4).

Indexes

0	–	total condition, settling chamber condition,	2	–	stator exit, rotor inlet,
			3	–	rotor exit,
1	–	stator inlet,	ax	–	axial component,

[1]German Aerospace Center (DLR), Institute of Fluid Mechanics, Bunsenstraße 10, D-37073 Göttingen, Germany

fl	–	time-resolved random fluctuation,
u	–	circumferential component,
w, $'$	–	relative frame of reference,
$\tilde{}$	–	ensemble-averaged value,
$\bar{}$	–	time-averaged value.

1. Introduction

In the past, most investigations of the actual efficiency of turbine blading were conducted in straight cascade facilities. Even though these tests provide valuable data, they are limited to two-dimensional flow. Furthermore, it is very difficult to simulate blade row interactions and other unsteady effects in these facilities. In order to satisfy the increasing demand for more information on three-dimensional and unsteady effects, full turbine stage tests have gained more and more importance in the last years.

The major disadvantage of stage tests is the fact, that the applicable measurement techniques are much more complicated and complex than those utilized in straight cascade tests. This is mainly due to the limited space between blade rows and the rotation of the rotor. For this reason it is rather difficult to maintain the accuracy of data that has been attained in two-dimensional investigations. A high degree of accuracy is however very important to be able to determine the source (stator or rotor) of certain effects.

One approach to determine flow quantities in the relative frame of reference (i.e. the rotor system) is the use of rotating probes. This technique requires however complicated mechanical set-ups and calibration procedures. Another approach is the determination of time-resolved data of the total pressure, the flow angle and the Mach number in the absolute frame of reference. The total pressure can be measured by utilizing probes equipped with fast response pressure transducers, while the Mach number and the flow angle can be determined by means of a Laser-2-Focus system (L2F). Even though the L2F measures only time-averaged values, proper triggering enables measurements of average velocities and average flow angles in fixed stator-rotor relative positions (see Kost, 1993). Thus, rotor wake 'traverses' can be conducted by triggering the system at different rotor positions. Assuming constant total temperature in the absolute frame, all properties of interest in the relative frame of reference can be computed from the time resolved total pressure, Mach number and flow angle in the absolute frame.

This paper describes time-resolved total pressure measurements downstream of a transonic high pressure turbine stage. Together with L2F measurements which will be conducted in the near future, the results will be used to determine the midspan flow field in the rotor system.

Another point of interest in this investigation was the effect of stator wakes on the total pressure distribution downstream of the rotor. As shown by many researchers (e.g. Arndt, 1991, Ladwig and Fottner, 1993 and Schröder, 1991) the wakes of upstream blade rows interact with downstream rows. In this case it was attempted to determine qualitative features of stator-rotor interactions in a high pressure turbine. The actual influence of these effects on the rotor losses can however not be determined without the above mentioned L2F results.

2. Experimental apparatus

Figures 1 and 2 show the layout and the circuit diagram of the wind-tunnel for rotating cascades at the DLR Göttingen (RGG). The RGG is a closed circuit continuously running wind-tunnel. A four stage radial compressor with a maximum pressure ratio of six, driven by a 1 MW DC-motor provides a volume flow rate of up to 15.5 m^3/s.

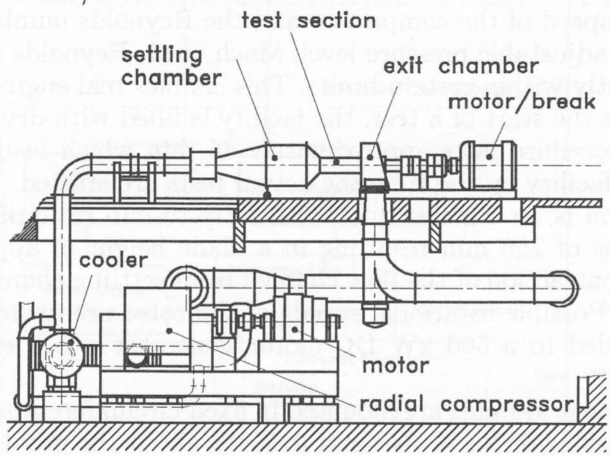

Fig. 1. Sketch of the RGG.

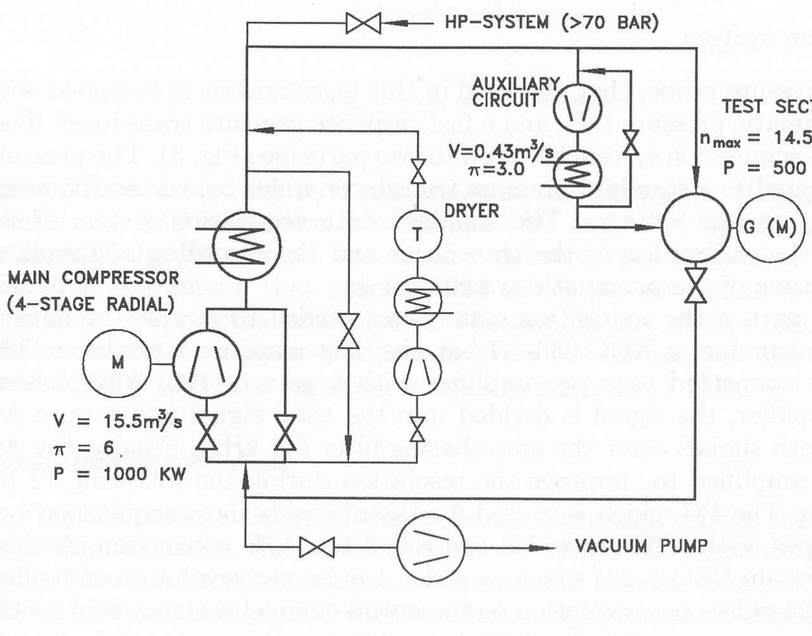

Fig. 2. Circuit diagram of the RGG.

A heat exchanger is located downstream of the compressor, enabling minimum total temperatures in the settling chamber of about 298 K. All components of the facility are controlled and monitored by means of a "Simatic S5" control system. The system keeps the pressure level in the facility within ±100 Pa, the temperature within ±0.3 K, and the rotational speed of the rotor within less than ±1 RPM.

Due to the fact, that the test section Mach numbers are mainly dependent on the rotational speed of the compressor and the Reynolds numbers are mainly dependent on the adjustable pressure level, Mach and Reynolds number can be varied independently within certain limits. This enables real engine conditions in the facility. Before the start of a test, the facility is filled with dry clean air. The entire start-up procedure lasts approximately 45 min which leads to adiabatic conditions in the facility by the time the actual tests are started.

The test section is an annular duct with a tip-to-hub ratio of typically 1.15 and a mean radius of 256 mm resulting in a blade height of approximately 36 mm. The entire contraction of the flow channel from settling chamber to cascade inlet is about 20. Possible rotational speeds of the rotor are up to 10,000 RPM. The rotor is coupled to a 500 kW DC-motor/generator which either drives or brakes it.

The probe carriage systems are mounted in fixed circumferential positions and allows radial traversing of the probes and rotation about the probe axes. In order to enable circumferential traverses behind a stator vane the stator can be rotated by approximately 18°.

Data acquisition system

The total pressure probe, that was used in this investigation is equipped with a common pneumatic pressure tube and a fast response pressure transducer. Therefore, the data acquisition system is split into two parts (see Fig. 3). The pressure tube was connected to a standard pressure transducer which converted the pneumatic informations into voltages. The standard data acquisition system of the RGG handled the calibration of the transducer and the recording of the data. The averaging time of the pneumatic system was 1s.

The second part of the acquisition system was needed to sample the data of the 'Kulite Semiconductor XQC-050-1.7 bar abs' fast response transducer. The transducer was connected to a pre-amplifier with a gain of 100. After having passed this amplifier, the signal is divided into the total signal and a pure AC signal before both signals enter the anti-aliasing filter (45 kHz). Finally, the AC signal is again amplified to improve the resolution during the following 12 bit A/D conversion. The PC which was used for the unsteady data acquisition system was equipped with software which controlled the A/D conversion. A shaft encoder (Heidenhain ERO 1324) which provided 1 pulse per revolution on its first channel and 1024 pulses per revolution on its second channel was mounted on the rotor shaft.

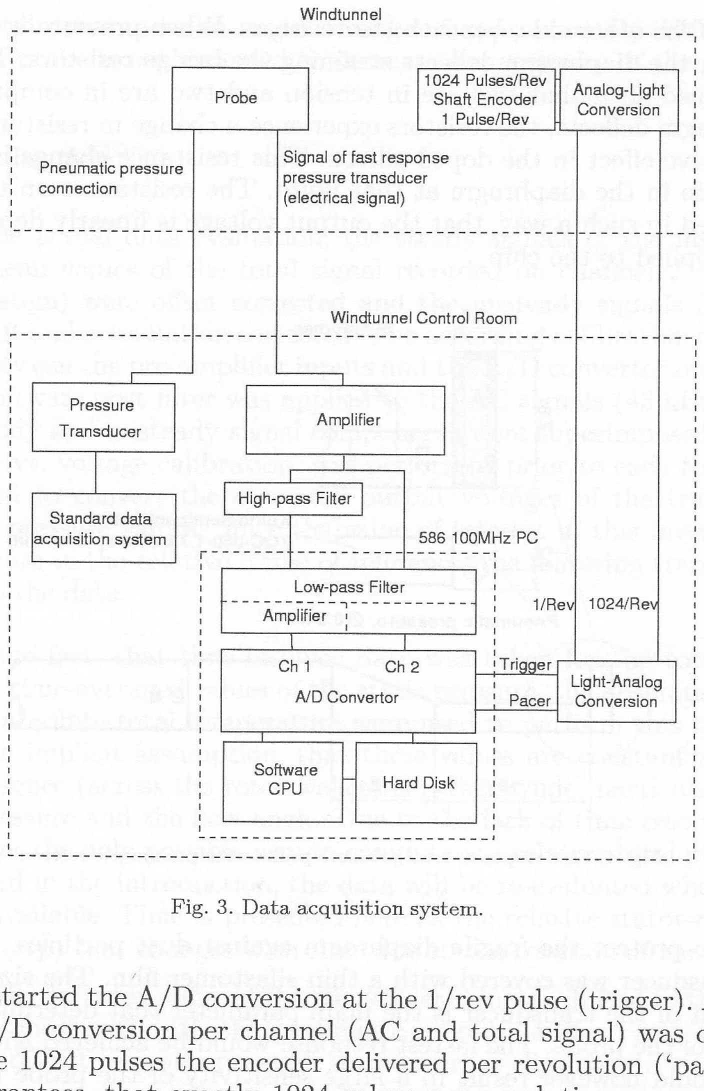

Fig. 3. Data acquisition system.

The software started the A/D conversion at the 1/rev pulse (trigger). After that, exactly one A/D conversion per channel (AC and total signal) was carried out for each of the 1024 pulses the encoder delivered per revolution ('pacer'). This technique guarantees, that exactly 1024 values per revolution are recorded, independent of the actual shaft speed. The samples are always taken at the same relative stator-rotor-probe position in every revolution. For the nominal rotor speed of 7894 RPM the resulting sampling rate is 134.7 kHz.

Measurement technique

Figure 4 shows a sketch of the probe that was used during this investigation. As mentioned above, this probe is equipped with a fast response pressure transducer. This semi-conductor pressure transducer consists of a silicon diaphragm bonded to a supporting pillar with a sealed cavity between. A Wheatstone resistor bridge is diffused into the upper surface of this diaphragm. Strain intensifiers are etched into the other side, beneath the resistors. When pressure is applied to the transducer, the diaphragm deflects straining the bridge resistors. These resistors are positioned such that two are in tension and two are in compression. When the diaphragm deflects, the resistors experience a change in resistance, due to the piezo-resistive effect in the doped silicon. This resistance change is proportional to the strain in the diaphragm at that point. The resistances on the diaphragm are arranged in such a way, that the output voltage is linearly dependent on the pressure applied to the chip.

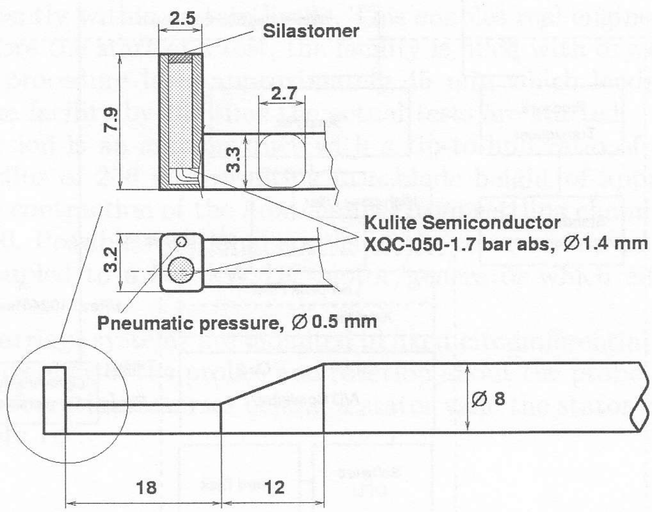

Fig. 4. Fast response total pressure probe with pneumatic reference.

In order to protect the fragile diaphragm against dust particles, the front part of the transducer was covered with a thin silastomer film. The size of the cavity in the front of the transducer is the main parameter that determines the cut-off frequency of the probe. The fastest response would be achieved with no cavity at all, this would however result in a large sensitivity of the probe to angular misadjustments. For this reason, the transducer was mounted into the probe with little recess. The cut-off frequency of this probe is sufficiently above the desired value of 50 kHz.

Unfortunately, the resistances of doped silicon are temperature dependent. Due to this fact, the mean value of the total pressure measured with a semi-conductor transducer tends to be rather inaccurate. In order to have an accurate reference mean value a standard pneumatic pressure tube was added to the probe.

The probe was mounted 0.5 axial rotor chords downstream of the rotor trailing edge at mid-span. It was turned to face the flow at the mean flow angle in the absolute frame of reference. This angle was determined with a standard wedge probe prior to the actual tests. Since Pitot probes are capable of measuring the correct total pressure in an angular range of approximately $\pm 10°$ the fixed position of the probe is not expected to decrease the accuracy of the data.

3. Data evaluation

Prior to the actual data evaluation, the steady signals of the fast response transducer (mean values of the total signal recorded on channel 2 of the data acquisition system) were offset corrected and the unsteady signals (channel 1) were phase shift and attenuation corrected. The according calibration curves were determined between the pre-amplifier inputs and the A/D convertor outputs. Furthermore, a software post filter was applied to the AC signals (43 kHz low-pass) before the steady and unsteady signal components were superimposed.

A pressure vs. voltage calibration, was performed prior to each test. The results were used to convert the corrected output voltages of the transducer to absolute total pressure values. Since the value of interest in this investigation is the total pressure in the relative frame of reference, the following transformation was applied to the data.

- Due to the fact, that time-resolved data was taken for the total pressure only, the time-averaged values of the static pressure, the absolute flow angle and the absolute total temperature were used to perform this transformation. The implicit assumption, that these values are constant around the circumference (across the rotor wakes) is rather crude, particularly for the static pressure and the flow angle. Due to the lack of time resolved data it is however the only possible way to compute the relative total pressure. As mentioned in the introduction, the data will be re-evaluated when the L2F data is available. Time is presented here as the relative stator-rotor-probe position (srp) that changes with time due to the rotation of the rotor.
- First of all, the mean value of the transducer signal is shifted to the pressure that was measured with the pneumatic pressure tube. Thus, the typical DC-shift of fast response pressure transducers is eliminated.
- The downstream Mach number

$$M_3(srp) = \sqrt{\frac{2}{\kappa - 1}\left[\left(\frac{p_{03}(srp)}{p_3}\right)^{\frac{\kappa-1}{\kappa}} - 1\right]}$$

- and the local speed of sound

$$a_3(srp) = \sqrt{\frac{\kappa R T_{03}}{1 + \frac{\kappa-1}{2} M_3^2(srp)}}$$

- lead to the velocity components in the absolute frame of reference:

$$c_{3ax}(srp) = \cos\alpha_3 \cdot M_3(srp) \cdot a_3(srp);$$

$$c_{3u}(srp) = \sin\alpha_3 \cdot M_3(srp) \cdot a_3(srp).$$

- Together with the known circumferential velocity of the rotor u_3, the velocity components in the relative frame are then given by:

$$w_{3ax}(srp) = c_{3ax}(srp); \quad w_{3u}(srp) = c_{3u}(srp) \; - \; u_3;$$

with: $(c_{3u} < 0)$.

- The Mach number in the relative frame

$$M_{w3}(srp) = a_3(srp) \cdot \sqrt{w_{3ax}^2(srp) + w_{3u}^2(srp)}$$

- finally leads to the relative total pressure

$$p'_{03}(srp) = p_3 \cdot \left(1 + \frac{\kappa - 1}{2} M_{w3}^2(srp)\right).$$

The following statistical procedures were then applied to the resulting relative total pressures:

- Ensemble averaging (EA)

$$\tilde{p}_i(srp_i) \; = \; \frac{1}{N} \sum_{j=1}^{N} p_{ij}(srp_i); \; i = 0...1023$$

  The EA procedure produces a signal that consists of 1024 points, corresponding to the encoder pulses which are averaged over N = 448 rotor revolutions.

- Determination of the EA random unsteadiness

$$p_{fl,i}(srp_i) \; = \sqrt{\frac{1}{N-1} \sum_{j=1}^{N} (p_{ij}(srp_i) - \tilde{p}_i(srp_i))^2}$$

  This procedure computes the root-mean-square value (RMS) at each of the 1024 rotor-probe positions.

- Time averaging

$$\bar{p} = \frac{1}{T} \int_0^T \tilde{p}(t)\, dt; \; (T = 448/7894RPM)$$

$$\text{random fluctuations} = \sqrt{\frac{1}{T}\int_0^T p_{fl}^2(t)\,dt}$$

$$\text{periodic fluctuations} = \sqrt{\frac{1}{T}\int_0^T (\tilde{p}(t) - \bar{p})^2\,dt}$$

(The periodic fluctuations are mainly wake-induced)

Finally, Fast Fourier Transforms of the EA pressure signal were computed.

4. Test parameters

During this investigation two different tests were carried out. The measurements were conducted with and without coolant ejection from the coolant slots close to the stator trailing edge at the pressure side. In the case with coolant, 3% of the main mass flow were ejected at the main flow temperature. The stator was turned during a test to vary the relative stator-probe position. Twelve different stator positions, covering approximately one stator pitch where investigated during each test.

The geometry of the stage and the parameters of the two test cases are listed in Tab. 1.

The terms inlet and exit refer to the rotor inlet and exit planes, respectively. All angles are given with respect to the axial direction. The cascade configuration and the probe position are shown in Fig. 5. All measurements were conducted at mid-span.

Table 1

Cascade geometry and test parameters

Geometry	Stator	Rotor
Chord c	49.92 mm	33.44 mm
Axial chord c_{ax}	29.86 mm	27.45 mm
Stagger angle	51.90 °	32.71 °
Number of blades	43	64
Stator / Rotor gap	14.6 mm	

Operating parameters	$c_m = 0\%$	$c_m = 3\%$
Relative inlet angle β_2	43.00 °	43.00 °
Relative exit angle β_3	-60.24 °	-60.84 °
Absolute exit angle α_3	-14.23 °	-15.07 °
M_{w2} (relative inlet)	0.41	0.41
M_{w3} (relative exit)	0.93	0.93
M_3 (absolute exit)	0.476	0.474
Re_{w2} (relative inlet)	0.24 E6	0.24 E6
M_2 (absolute inlet)	1.0	1.0
Rotor speed	7894 RPM	7894 RPM
T-T pressure ratio	2.65	2.64

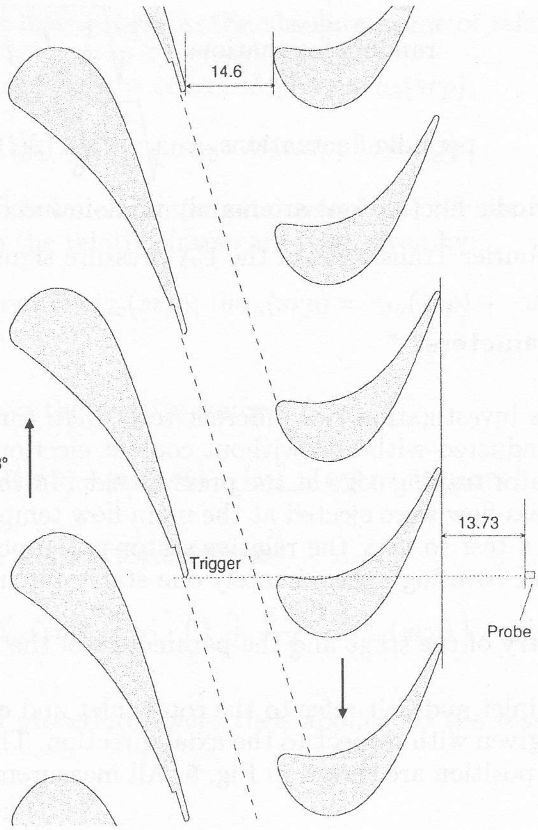

Fig. 5. Stage configuration.

5. Results and discussion

Time-averaged values

The time-averaged pressure and fluctuation values downstream of the rotor are plotted in Fig. 6 for the case with no coolant ejection, and the distributions of these parameters for the 3% coolant ejection case are given in Fig. 7. The top plot in both figures shows the absolute total pressure data of the pneumatic pressure tube and the fast response transducer (DC reading). The difference between these two curves, is mainly due to the above-mentioned offset shift of semi-conductor pressure transducers. The center plots show the total pressure data transformed into the relative frame of reference. Finally, the periodic fluctuations (periodic with respect to rotor wake passages) and the random fluctuations (RMS values) are given in the bottom plots of Fig. 6 and 7. All these time-averaged data sets are plotted versus stator pitches, i.e. every data point represents one of the investigated 12 stator positions (the stator was moved, while the probe remained in a fixed circumferential position).

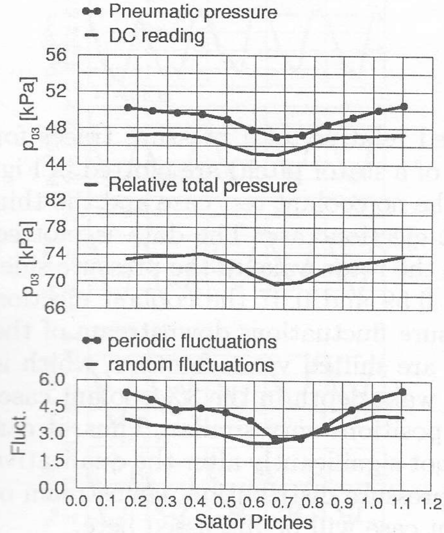

Fig. 6. Time-averaged values, $c_m = 0\%$.

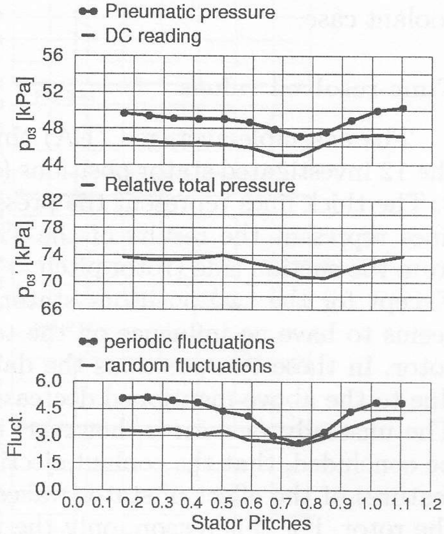

Fig. 7. Time-averaged values, $c_m = 3\%$.

The absolute as well as the relative total pressure traces in Fig. 6 clearly indicate the influence of the stator on the downstream total pressure distribution. The wake shed by the stator results in a wide flat wake in the downstream pressure distributions between stator pitch = 0.4 and stator pitch = 1.0. The resulting parameters that originate from the stator suction side are plotted to the left of this wake, while the pressure side parameters are plotted to the right. The periodic fluctuations (mainly due to the amplitude of the relative total pressure fluctuations of the rotor) in the center of the stator wake effect are decreased by almost 50 % with respect to the periodic fluctuation level outside the wake effect. The random fluctuations, which are due to non-periodic effects such as wake-mixing processes show a similar behaviour. However, these values are only about half as much influenced by the stator wake as the periodic fluctuations are. Note, that the turbulent time scale in typical RGG cascades is in the order of 300 kHz. Therefore the probe data which was low-pass filtered at 45 kHz certainly does not resolve any kind of turbulent fluctuations. Thus the random fluctuations are solely due to non-periodic non-turbulent effects.

The time averaged values for the test case where 3% of the main mass flow were ejected from the coolant slots close to the stator trailing edge show a pattern similar to that of the time-averaged data for the no coolant case (see Fig.

7). The effect of the stator wake on the rotor downstream pressure distribution is however less pronounced. Taking into account that the simulated coolant 'fills up' the stator wake, it is not surprising that the effect of the resulting flat stator wake on the rotor wakes is smaller than that of the deeper stator wake in the no coolant case.

Time-resolved values

The ensemble-averaged (EA) time-resolved relative total pressure traces for the 12 investigated stator positions (Pos = % of a stator pitch) are plotted in Fig. 8. The thick lines represent the pressures of the no coolant test case and the thin lines represent the results of the 3% coolant ejection case. The data is plotted from the suction side (rotor pitch = 0) across the rotor wake to the pressure side. Except for the two positions stator pitch = 0.59 and 0.67 the coolant ejection seems to have no influence on the total pressure fluctuations downstream of the rotor. In these two positions the data traces are shifted vs. each other, which is due to the above-mentioned decreased stator wake depth in the 3% coolant case. The unsteady pattern is, however, in all 12 positions very similar. Thus, it can be concluded, that the coolant ejection does not significantly alter the qualitative features of the effect of stator wakes on the pressure distribution downstream of the rotor. For this reason, only the no coolant case will be discussed here.

As already mentioned in the discussion of the time-averaged values, the pressure amplitudes of the signals measured in stator-probe relative positions outside the stator wake effect are significantly larger than those measured in positions where the stator wake effects the rotor pressure distribution. Fig. 8 indicates a continuous decay of the rotor wake depth from position 0.17 (top plot) to position 0.67. At the same time the width of the relative total pressure maxima decreases, which means, that the rotor wake width increases. Both effects are reversed between position 0.67 and position 1.10. The continuous decay of the pressure amplitude between position 0.17 and 0.67 and its increase between position 0.67 and 1.10 can also be seen in the amplitude spectra of the relative total pressures in Fig. 9.

Since from the plots of the time-averaged data the stator wake effect on the rotor pressure distribution was identified between position 0.4 and 1.0 with the maximum effect being close to position 0.7, it can be concluded, that the stator wake damps the rotor pressure fluctuations. Due to the fact, that the rotor wake width increases while its depth decreases, this conclusion does not necessarily mean, that the rotor losses are decreased under the influence of the stator wake. In order to accurately compute the rotor pressure losses in the relative frame of reference time-resolved static pressure and flow angle signals have to be determined. For this reason, the L2F measurements which are described in the introduction will be used to re-evaluate the data presented here.

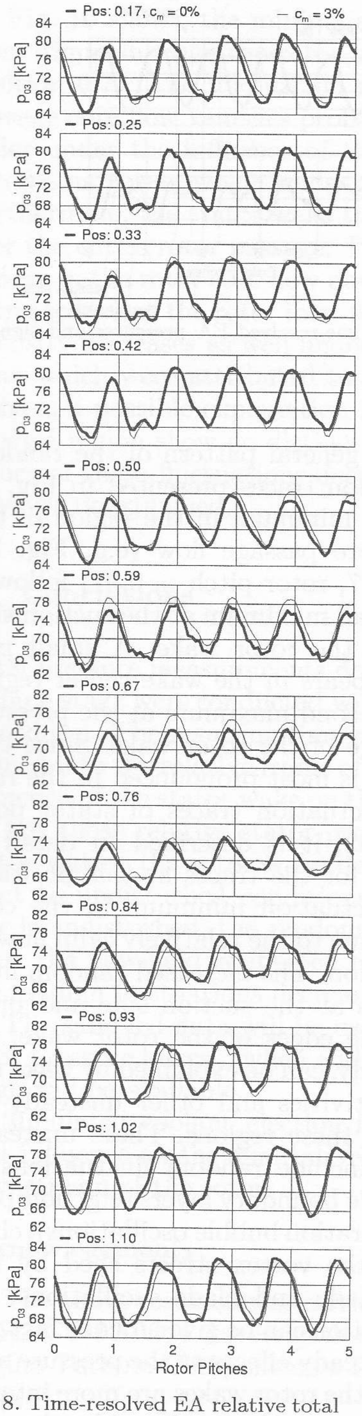

Fig. 8. Time-resolved EA relative total pressures, $c_m = 0\%$(—), $c_m = 3\%$(—).

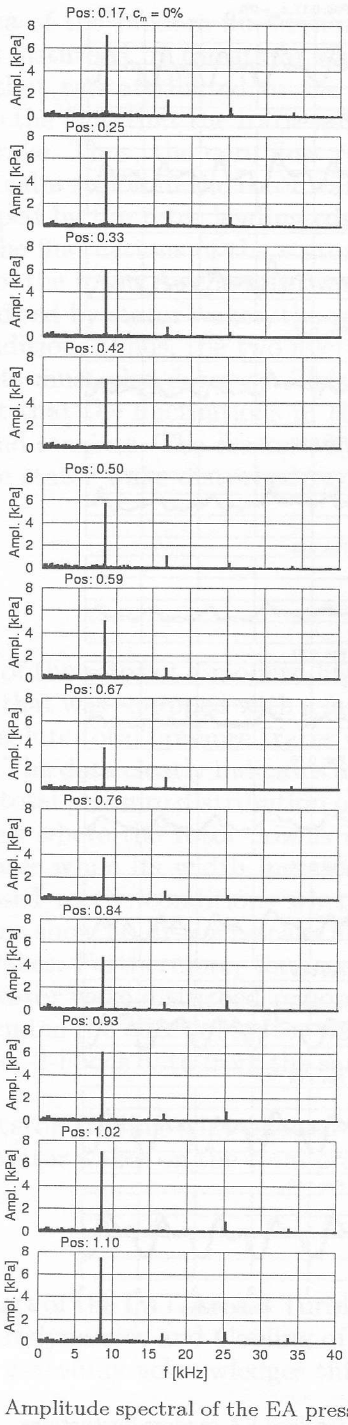

Fig. 9. Amplitude spectral of the EA pressure signals, $c_m = 0\%$.

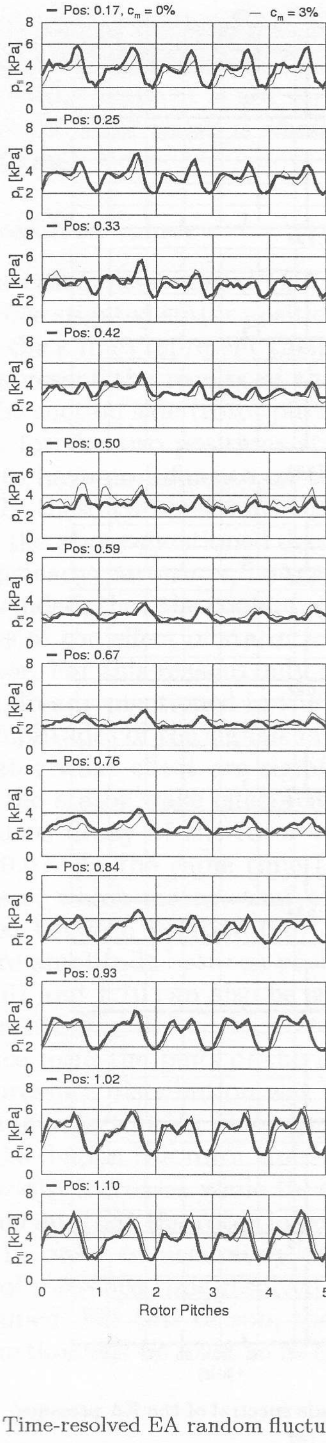

Fig. 10. Time-resolved EA random fluctuations, $c_m = 0\%$(—), $c_m = 3\%$(—).

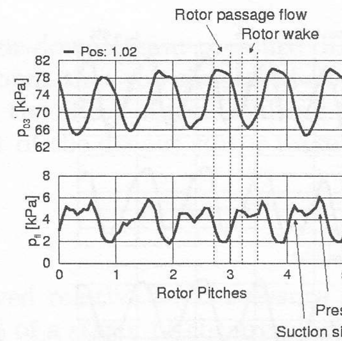

Fig. 11. Time-resolved EA pressures and signals, $c_m = 0\%$.

The general pattern of the random fluctuation traces presented in Fig. 10 shows a minimum in the region of the rotor core passage flow (e.g. Fig. 10, Pos: 0.17, rotor pitch = 0.91) followed by a small maximum at the suction side edge of the rotor wake. A small plateau appears in the wake center region and a second maximum at the pressure side edge of the rotor wake. Since this pattern is most pronounced in the random fluctuation traces of stator position 1.02, it is described in detail in Fig. 11 for the traces at this position. The fluctuation minimum in the core flow is due to the relatively calm flow in this region. The increased random fluctuations at the suction side and pressure side edges of the rotor wake, respectively, can be explained by wake mixing activities and other unsteady effects in these regions. These unsteady effects include random fluctuations in the blade boundary layers (e.g. non-periodic separation bubble oscillations), changes in the vortex streets shed by the rotor blade and blade oscillations. No explanation can be given for the fact, that the unsteady effects at the pressure side edge of the rotor wakes are more intense than those at the suction side edge.

As Fig. 10 shows, the minima and maxima of the random fluctuation traces almost diminish when the rotor inlet flow is disturbed by the stator wake (around position 0.7). The fluctuation minimum that was attributed to the calm rotor passage core flow vanishes probably due to the fact, that the rotor wake becomes wider under the influence of the stator wake. Thus, the core flow region must become narrower, which leads to a smaller calm region in the rotor wake traverse. Furthermore, the stator wake that is chopped by the rotor leading edges extends over the entire rotor passage. Therefore, the fluctuations of the stator wake flow appear in the rotor core flow downstream of the rotor. As the rotor wake depth is decreased when the rotor inlet flow is disturbed by stator wakes, the wake mixing intensity decreases as well under these conditions. Thus, the two fluctuation maxima which were attributed to these effects must also decrease. This discussion delivers a possible explanation for the fact that the fluctuations in the wake disturbed region show no distinct minima and maxima. The reason why the mean values of these fluctuations decrease in the stator wake disturbed region remain however unexplained.

6. Conclusions

Total pressure measurements downstream of the rotor of a modern high-pressure turbine stage were conducted with a probe that was equipped with a fast response transducer. The resulting time-resolved absolute total pressure traces were transformed into the relative frame of reference. The data clearly indicates a significant influence of the stator wake on the relative total pressure distribution of the rotor.

For those relative stator-probe positions where the rotor flow is affected by stator wakes, the rotor wake depth decreases while its width increases with respect to undisturbed conditions. As opposed to the conditions when the rotor flow is undisturbed, the random fluctuations show no distinct peaks and minima when the flow-field is affected by stator wakes. Furthermore, the mean value of the random fluctuations decreases in the stator wake disturbed region.

The sampled data will be used to determine the effect of stator wakes on the rotor pressure losses, when additional Laser-2-Focus data from the same turbine stage will be available.

Simulated coolant ejection from the stator trailing edge showed no significant influence on the qualitative effects of stator wakes on the total pressure field downstream of the rotor.

Acknowlegements

The above research was carried out as part of the IMT Area 3 Turbine Project AER2-CT-92-0044 'Investigation of the Aerodynamics and Cooling of Advanced Engine Turbine Components'. The author gratefully acknowledges this financial support.

Manuscript received in March 1998

References

[1] ARNDT N.: *Blade row interaction in a multistage low-pressure turbine*, ASME-Paper 91-GT-283.

[2] KOST F.: *Improvements in the application of laser-two-focus velocimetry to transonic rotor flows*, Proc. of the 13th Symposium on *Measurement Techniques for Transonic and Supersomic Flows in Cascades and Turbomachines*, Zürich, Switzerland 1996.

[3] LADWIG M., FOTTNER L.: *Experimental investigations of the influence of incoming wakes on the losses of a linear cascade*, ASME-Paer 93-GT-394.

[4] SCHRÖDER TH.: *Investigations of blade row interaction and boundary layer transition phenomena in a multistage aero engine low-pressure turbine by measurements with hot-film probes and surface-mounted hot-film gauges*, von Karman Institute for Fluid Mechanics, 1990-1991 Lecture Series.

Efekty wpływu śladu za stojanem na rozkład ciśnienia całkowitego za wirnikiem turbiny transonicznej

Streszczenie

W ramach projektu europejskiego, nakierowanego na badania oddziaływań opływu stojana i łopatek wirnika, przeprowadzono pomiary w celu wyznaczenia nieustalonego rozkładu ciśnienia za częścią wysokociśnieniową turbiny transonicznej. Badania przeprowadzono w tunelu powietrznym dla obracającej się kaskady, w laboratorium DLR w Getyndze (RGG). Jest to stanowisko z zamkniętą pętlą, które umożliwia badania w stopniu turbiny dla rzeczywistych liczb Macha i Reynoldsa. Łopatki stojana posiadały szczeliny do pozbywania się chłodziwa, blisko krawędzi spływu na stronie ciśnieniowej. Rurkę Pitota posiadająca szybki przetwornik ciśnienia oraz zwykłą rurkę pneumatyczną zamontowano za wirnikiem. Pomiar odbywał się w odległości 0.5 cięciwy osiowej wirnika, za krawędzią spływu wirnika. Pośród wartości średnich całkowitego ciśnienia za stopniem wyraźnie widoczny jest ślad za stojanem. Okresowe fluktuacje całkowitego ciśnienia za wirnikiem są około 50% mniejsze w obszarze śladu stojana, niż w obszarze niezakłóconego przepływu na wlocie. Dlatego ślad za stojanem tłumi fluktuacje ciśnienia całkowitego generowane przez wirnik.